Nuclear Inst. and Methods in Physics Research, A 966 (2020) 163858

Contents lists available at ScienceDirect

Nuclear Inst. and Methods in Physics Research, A

journal homepage: www.elsevier.com/locate/nima

# Wide-angle transmission analyzer for polarized neutrons using equiangular spirals

Peter Böni [a,b,*], Christian Schanzer [b], Michael Schneider [b]

[a] Physics Department E21, Technical University of Munich, D-85748 Garching, Germany
[b] SwissNeutronics AG, Brühlstrasse 28, CH-5313 Klingnau, Switzerland

ARTICLE INFO

*Keywords:*
Polarized neutrons
Neutron scattering
Supermirror
Guides

ABSTRACT

Much progress in neutron spectroscopy has been achieved with the invention of direct geometry time-of-flight (TOF) spectrometers, which allow an efficient determination of the scattering function $S(\mathbf{Q}, E)$ over large ranges in momentum $\mathbf{Q}$ and energy $E$. For separating (i) magnetic from nuclear and (ii) incoherent from coherent scattering, polarization analysis of the scattered neutrons is often required. Typically, the polarization is analyzed by means of $^3$He spin filters or by curved magnetized mirrors, which are arranged radially around the sample reflecting the spin-up neutrons while the spin-down neutrons are absorbed. In the following we describe the design of a wide-angle polarization analyzer that uses polarizing mirrors with an equiangular profile in transmission, i.e. the spin-down neutrons are transmitted to the detector while the spin-up neutrons are reflected and finally absorbed. Because of the almost constant angle of reflection the bandwidth is large, i.e. it is given by the ratio $Q_P = m_{max}/m_{min}$, where $m_{max}$ and $m_{min} \simeq 0.68$ are the maximum and minimum useful $m$-values of the polarizing supermirror. For small samples and $m_{max} = 5$, $Q_P = 7.4$ is achieved. The proposed design eliminates the significant losses of neutrons due to absorption by the front faces of the polarizing blades of wide-angle analyzers in reflection. Moreover, in transmission, the phase space of the neutrons is barely affected by the mirrors and the polarization is rather constant.

## 1. Introduction

Since the seminal work of Moon, Riste, and Koehler [1], polarization analysis of neutrons has been established to be a unique and powerful method for the investigation of the static and dynamic properties of condensed matter. It allows separating magnetic from nuclear scattering and to distinguish between coherent and incoherent scattering, for example in hydrogen containing materials. Originally, inelastic neutron scattering experiments were performed using triple-axis spectrometers [2,3]. Here, Heusler monochromators provided an efficient means to polarize, analyze, as well as to define the energy of the incident and scattered neutrons.

Another means to polarize neutrons are bending devices [4] using polarizing supermirrors [5,6]. Supermirror based beam devices have the advantage that neutrons can be reflected over a large range of energy [7]. Therefore, they are particularly well suited for direct time-of-flight (TOF) spectrometers, which offer the unique advantage of delivering data over a large range of momentum, $\mathbf{Q}$, and energy, $E$, transfer.

The first implementation of supermirror for the analysis of the polarization of the scattered neutrons over a large solid angle was realized by Schärpf at the TOF spectrometer D7 at the ILL [8] and Schweika and Böni at the spectrometer for diffuse neutron scattering (DNS) at the former Jülich research reactor and now at MLZ in Garching [9]. TOF spectrometers are particularly powerful at pulsed spallation sources such as SNS [10], target stations TS1 and TS2 at ISIS [11], MLF at J-PARC [12], and the future ESS [13] in Lund. To allow a highly efficient polarization analysis over the large solid angles offered by the large detector banks and to extend the energy range of the spectrometers new concepts for polarization analysis have to be developed.

One way to analyze the polarization over a wide range of angles can be realized by $^3$He spin filter cells [14], which can be placed around the sample. Although this technique provides a reasonably high polarization, the cells have to be regenerated periodically. Moreover, the cells are highly sensitive to gradients of magnetic fields thus making an application close to high magnetic fields difficult. Last but not least, these systems require a high degree of maintenance, which makes their operation rather demanding. In passing we note that also supermirror based devices may suffer in performance if exposed to the strong stray fields of non-compensated superconducting magnets.

In contrast, wide-angle polarization analysis using supermirror is a very robust technique and does not require maintenance. The basic principle of a wide-angle polarization analyzer (WAPA) is shown

* Corresponding author at: Physics Department E21, Technical University of Munich, D-85748 Garching, Germany.
*E-mail address:* peter.boeni@frm2.tum.de (P. Böni).

https://doi.org/10.1016/j.nima.2020.163858
Received 29 January 2020; Received in revised form 25 March 2020; Accepted 26 March 2020
Available online 1 April 2020
0168-9002/

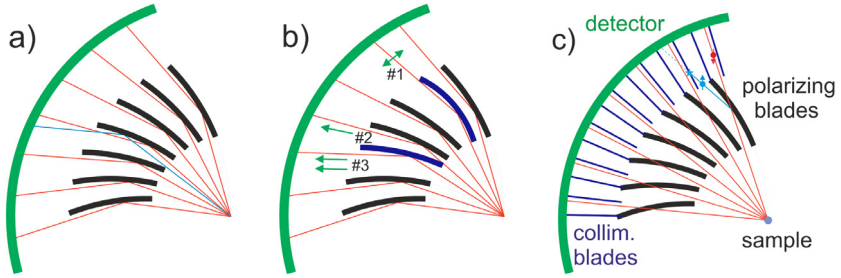


**Fig. 1.** Design of wide-angle polarizing analyzers (WAPAs) in reflection and transmission geometry. (a) shows the geometry of a reflecting WAPA as realized at the beamlines HYSPEC at SNS and POLANO at J-PARC. (b) Warping of the polarizing blades (thick solid lines in black) along the flight direction of the neutrons reduces the angular resolution (beam #1). Warping in the vertical direction induces variations of the width of the channels (beams #2 and #3) leading to variations in intensity for various scattering angles. (c) WAPAs in transmission geometry do not affect the phase space of the transmitted neutrons. The Si-blades are essentially transparent for the neutrons. Neutrons with the wrong polarization are absorbed by a collimator that is placed between the WAPA and the detector (beam path in blue). (For interpretation of the references to color in this figure legend, the reader is referred to the web version of this article.)

in Fig. 1 (a). Circularly bent blades made from neutron-absorbing glass and coated with polarizing supermirror are arranged around the sample. Neutrons entering the channels between the polarizing blades are transmitted to the detector and polarized with spin up while the neutrons with spin down are transmitted through the supermirror and absorbed in the boron containing glass.

WAPAs in reflection geometry have been installed recently at the TOF spectrometers HYSPEC [15,16] at SNS and POLANO [17–20] at MLF covering a range of scattering angles of the order of $60^0$. They are also used as polarization analyzers in neutron spin echo spectroscopy [21,22]. However, the reflection geometry involves some serious drawbacks: First of all, neutrons hitting the front face of the blades (thick black lines in Fig. 1) are lost. For example, the width of the channels of the WAPA for POLANO at the entrance is 0.6 mm and the thickness of the blades is 0.3 mm [20]. Therefore, even in the ideal case only 66% of the correctly polarized neutrons can reach the detector. Further losses occur due to the finite reflectivity of the supermirrors. In addition, the transmission is reduced by warping of the blades in the longitudinal (beam #1) and vertical direction (beams #2 and #3) as sketched in Fig. 1(b).

In this work we discuss the realization of a wide-angle analyzer using polarizing blades made from Si-wafers in a transmission geometry (tWAPA) as shown in Fig. 1(c). The major advantages are that (i) the phase space of the neutrons is essentially preserved, (ii) shading of the neutron beam by the front face of the blades is avoided, and (iii) the waviness of the blades only marginally affects the trajectories of the neutrons scattered by the sample.

## 2. tWAPA using Z-cavities

Two-dimensional spin analyzers in transmission geometry have already been realized by Krist many years ago [23]. The basic idea is to arrange Z-cavities radially around the sample position as shown on the left hand side of Fig. 2. The cavities are separated by absorbing blades, which are intersected with silicon wafers that are coated with polarizing supermirror. Typical spin-dependent transmission curves of a silicon wafer that is coated on both sides with Fe/Si polarizing supermirror with $m = 5$ are shown in Fig. 3. $m = 1$ corresponds to the angle of total reflection of a Ni-coating. The double-sided coating increases the reflectivity of 72% of a single coating (at $m = 5$) to 90%.

The high reflectivity of FeSi mirrors yields in transmission a high polarization $P \geq 90\%$ between the critical edge $m_{min} \simeq 0.68$ (spin down and spin up) and the critical edge $m_{max} = 5$ (spin up). Therefore, neutrons are polarized within an angular range given by

$$\theta_c^{dn} = cm_{min}\lambda \leq \theta_c^{up} = cm_{max}\lambda, \tag{1}$$

where $\lambda$ designates the wavelength of the neutrons and the constant $c$ is given by $c = 0.00173$ rad/Å ($c = 0.099°$/Å). In terms of wavelength at a fixed angle of incidence $\psi$, neutrons within a range

$$\lambda_{min} = \frac{\psi}{cm_{max}} \leq \lambda \leq \lambda_{max} = \frac{\psi}{cm_{min}} \tag{2}$$

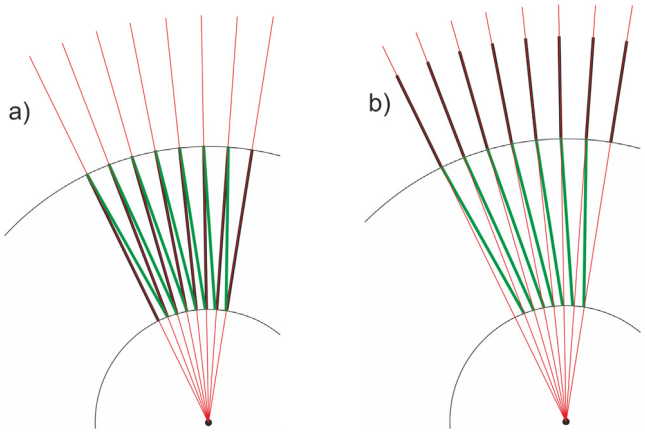


**Fig. 2.** (a) Design of a WAPA using Z-cavities (green lines) that are arranged radially around the sample position [23]. The channels are separated by absorbing blades (black lines). (b) The flexibility of the tWAPA may be increased and the complexity of the device reduced by arranging the absorbing blades downstream of the polarizing supermirrors. The radially emerging lines shown in red indicate beam trajectories. (For interpretation of the references to color in this figure legend, the reader is referred to the web version of this article.)

become polarized. The angle $\psi$ is chosen to be close to $\theta_c^{up}$. The suppression of neutrons with $\lambda > \lambda_{max}$ may be helpful for avoiding frame overlap in TOF spectroscopy.

Because of the finite thickness of the required absorbing blades ($t \simeq 0.3$ mm), the transmission is still impaired by the absorption of neutrons by the front face of these blades similarly as for the WAPA in reflection geometry. We propose improving the design by replacing the absorbing blades within the polarizing device by a radial collimator that is placed around the polarizing device as shown at the right hand side of Fig. 2. The absorbing Mylar foils of the collimator have a thickness of typically 75 μm. Therefore, the transmission losses are strongly reduced. Moreover, the separation of polarizer and collimator allows the collimation to be varied according to the requirements of the experiment. Last but not least, the length of the collimating section can be reduced by increasing the number of mylar foils.

In Appendix A we have evaluated the properties of a tWAPA that is composed of Z-cavities as shown on the right hand side of Fig. 2. The calculations show that the tWAPA is able to yield a good performance over a range of wavelengths $\lambda_{min} \leq \lambda \leq \lambda_{max}$ where the parameter for the bandwidth

$$Q_P = \frac{\gamma_{min} m_{max}}{\beta_{max} m_{min}} \tag{3}$$

provides a measure for the dynamic range of the tWAPA. Here, $\gamma_{min}$ and $\beta_{max}$ designate the minimum and maximum angle of reflection of

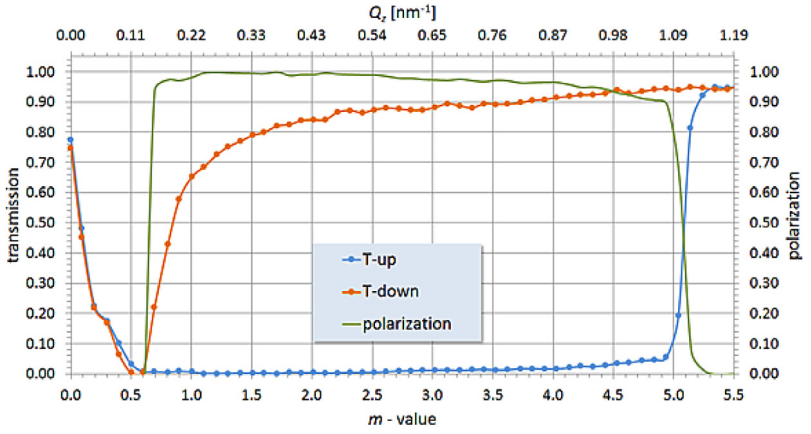


**Fig. 3.** Measured spin-dependent transmission (orange and blue lines) and polarization (green line) of an Fe/Si polarizing supermirror with $m = 5.0$ on Si-wafer that has a thickness $t = 0.3$ mm. The wafers are coated on both sides. The polarization of the transmitted beam, $P_{trans} > 90\%$, is high due to the high reflectivity of the supermirror [24]. (For interpretation of the references to color in this figure legend, the reader is referred to the web version of this article.)

neutrons hitting the polarizing blades. The angles are given by the geometry of the tWAPA (see Fig. A.7). The supermirror parameters $m_{min}$ and $m_{max}$ are taken from the transmission measurements of the supermirror such as shown in Fig. 3 yielding $m_{min} = 0.68$ and $m_{max}$ (here $m_{max} = 5$).

There are several drawbacks in the design of the tWAPA using flat substrates that should be eliminated. First of all, Eq. (3) implies that the wavelength band is reduced if $\gamma_{min}$ is significantly smaller than $\beta_{max}$. Note that $m_{max}/m_{min}$ is fixed by the supermirror coating. Secondly, the collimating blades become quite lengthy to warrant the removal of all wrongly polarized neutrons. This is particularly true for neutrons hitting the blades under small angles. Thirdly, warping of the Si wafers along the beam direction affects the transmitted neutron beams in particular those hitting the substrates under small angles $\gamma_{min}$. The obvious solution to circumvent these drawbacks is the use of equiangular spirals, which are introduced in the next paragraph.

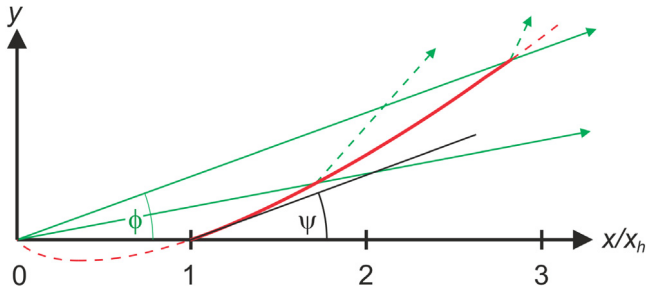


**Fig. 4.** The equiangular spiral has the property that all beams emerging from the origin (green lines with arrows) intersect the spiral (red line) under a fixed angle $\psi$. For polarization analysis the section indicated by the thick solid line in red is used. (For interpretation of the references to color in this figure legend, the reader is referred to the web version of this article.)

## 3. tWAPA using equiangular spirals

As pointed out by Stahn and Glavic, a neutron beam should intersect a polarizing supermirror ideally everywhere under an identical angle of reflection $\psi$ [25]. For a parallel beam, this condition is fulfilled by using flat polarizing mirrors. They are typically used as polarizing elements in V- and Z-cavities (see Section 2) [26]. For focused beams, the corresponding surfaces turn out to have the shape of an equiangular spiral [25]. Therefore, the optimum profile of the polarizing mirrors for a wide-angle analyzer are equiangular spirals too. This conclusion is supported by taking a closer look at Eq. (3): For an equiangular spiral, $\gamma_{min}/\beta_{max}$ approaches 1 thus increasing the useful wavelength band, i.e. $Q_P \rightarrow m_{max}/m_{min}$, when compared with a tWAPA using Z-cavities. To get rid of the unwanted spin-up neutrons, a radial collimator must be placed at the exit of the analyzer similarly as for the tWAPA using Z-cavities.

For reasonably small samples, the wavelength band of the transmitted polarized neutrons is now given for fixed $\psi$ by Eq. (2). According to Fig. 4 we introduce the salient parameters of the equiangular spiral. In polar coordinates $(r, \phi)$, its shape can be expressed by

$$r(\phi) = x_h e^{k\phi}, \tag{4}$$

where $k = 1/\tan\psi$ designates the slope of the spiral at the position $r(0) = x_h$ with respect to the $x$-axis and $\phi$ corresponds to the angle between the $x$-axis and the intersecting beam (green lines with arrows).

In Cartesian coordinates one obtains

$$x = x_h e^{\phi/\tan\psi} \cos\phi \tag{5}$$

$$y = x_h e^{\phi/\tan\psi} \sin\phi. \tag{6}$$

Eq. (4) can be rewritten in the following form

$$\ln\frac{r}{x_h} = \frac{\phi}{\tan\psi}. \tag{7}$$

For small angles $\psi \ll 1$ it can be approximated by

$$\phi \simeq \psi \ln\frac{x}{x_h}. \tag{8}$$

The proposed implementation of equiangular spirals in the polarizing device is shown in Fig. 5. Inserting the geometrical parameters $x_h = R_1$, $x = R_2$ and $\psi = \theta_c^{up}$ in Eq. (8) and assuming the sample position to be at the origin $(0, 0)$ we obtain for the width of the channels at the entrance and the exit of the WAPA

$$w \simeq \phi R_1 = \theta_c^{up} R_1 \ln\frac{R_2}{R_1} \tag{9}$$

$$W \simeq \phi R_2 = \theta_c^{up} R_2 \ln\frac{R_2}{R_1}. \tag{10}$$

For cylindrical samples with a small diameter, $d \simeq 0$, the angle of reflection is strictly $\psi \simeq \theta_c^{up}$, i.e. there is a well defined wavelength $\lambda_{min}$ (Eq. (2)) below which the analyzer does not polarize the incident neutrons. The upper useful wavelength is given by $\lambda_{max}$ (Eq. (2)) above which all neutrons are totally reflected (Fig. 3). The sharp cutoffs are in contrast to a WAPA using flat substrates, where the wavelength dependence of the polarization is more gradual thus reducing the bandwidth parameter $Q_P$.

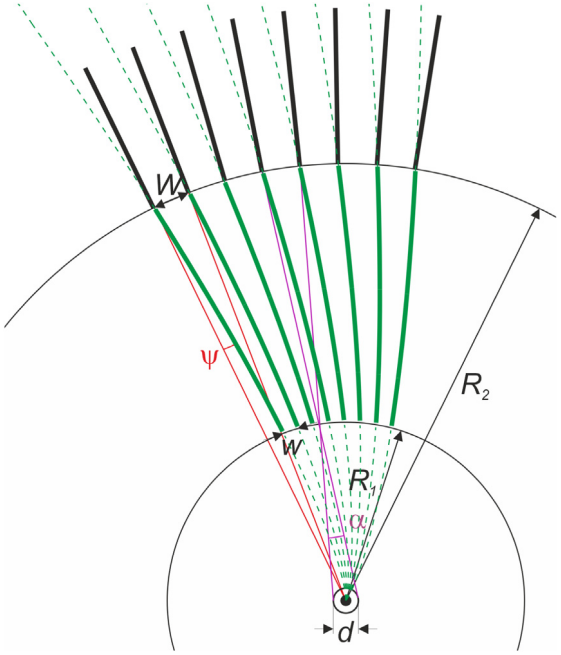


**Fig. 5.** Neutron beams emerging from the center of the sample hit the surface of the spirals everywhere under an identical angle $\psi$ if the profile is given by an equiangular spiral. $\psi$ is typically chosen to assume values close to $\theta_c^{up}$. For samples with a finite size, the reflection angle is spread over an interval $\alpha$.

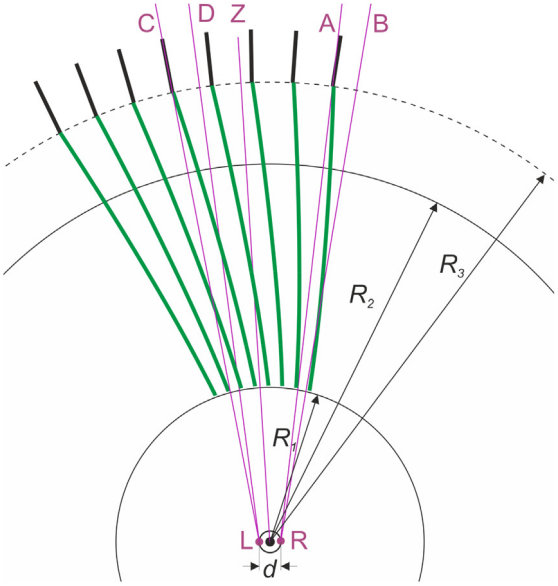


**Fig. 6.** To make sure that all neutrons emerging from a sample with $d > 0$ hit the polarizing blades, the equiangular spirals are extended towards the detector thus ending on a circle with radius $R_3$ (dashed circular line). Neutrons with spin-up emerging from point R (beams A and B) will now hit the polarizing blades under a smaller angle of reflection thus reducing the upper critical wavelength. In contrast, neutrons emerging from L (beams C and D) are reflected under a larger angle thus increasing the lower critical wavelength.

We have shown that the mathematics for the design of a tWAPA with equiangular spirals is straightforward for samples with a diameter $d = 0$. To allow an efficient polarization analysis for samples with $d > 0$ we propose a simple modification of the design. As shown in Fig. 6, neutrons scattered near the position R of the sample can leave the analyzer without intersecting the polarizing blades. Therefore, their polarization is not analyzed. A simple remedy is the extension of the equiangular spirals towards the detector. Now, all neutrons scattered by the sample intersect the polarizing blades once or twice and are potentially analyzed. Neutrons intersecting two blades have an improved polarization.

However, the performance of the tWAPA is nevertheless impaired because its bandwidth decreases with increasing $d$ due to two effects: Firstly, neutrons emerging from R impinge the polarizing mirrors under an angle of reflection $\psi_R = \psi - \alpha/2$. Therefore, according to Eq. (2), neutrons with spin-down are already reflected at a smaller wavelength, i.e. $\lambda_R < \lambda_{max}$. Secondly, neutrons emerging from point L hit the polarizing blades under an angle $\psi_L = \psi + \alpha/2$. Therefore, according to Eq. (2), the lower critical wavelength is increased, i.e. $\lambda_L > \lambda_{min}$. As a result, the parameter for the bandwidth, $Q_P$, is reduced. To make sure that all transmitted neutrons are polarized, the divergence of the scattered neutrons has to be reduced by a tighter collimation leading to an intensity loss of approximately $\alpha/\psi$. Of course, the reduction of the wavelength band with increasing sample size is a generic drawback of WAPAs based on supermirror technology.

A major feature of a WAPA operated in transmission is the possibility to adjust the angular resolution of the analyzer without affecting the polarizing section. The angular resolution of the transmitted neutrons can be adapted by inserting an appropriate radial collimator at the exit of the analyzer. Note that the length of the collimating section can be reduced strongly by increasing the number of channels $N_{coll}$ when compared with the number of equiangular spirals $N_{spir}$.

Finally, we compare the performance of the tWAPA with a $^3$He spin filter cell. According to Heil et al. [27], the opacity of a cell is given by

$$k = \sigma_c N l = 0.0732 \cdot \lambda[\text{Å}]\, p[\text{bar}]\, l[\text{cm}]. \tag{11}$$

Here, $\sigma_c$, $N$, $l$, and $p$ designate the capture cross section of $^3$He, the density of the $^3$He nuclei, the thickness of the cell, and the pressure of the $^3$He gas, respectively. The polarization and the transmission of an initially unpolarized beam are given by

$$P(\lambda) = \tanh\left(k P_{He}\right), \tag{12}$$

$$T(\lambda) = e^{-k}\cosh\left(k P_{He}\right), \tag{13}$$

where $P_{He}$ is the polarization of the $^3$He.

We compare in Table 1 the performance of a $^3$He cell with a tWAPA for wavelengths in the range 2 Å $\leq \lambda \leq$ 14.8 Å corresponding to $Q_P = 7.4$. Note that the parameter $Q_P$ is solely determined by the $m$-value of the supermirror and independent of the dimensions of the WAPA. In analogy to existing WAPAs, a typical tWAPA will cover an angular range of $60^0$ and will have radii $R_1 = 500$ mm and $R_2 = 750$ mm. The parameters of the $^3$He cell are: $l = 3$ cm, $p = 2.5$ bar, and $P_{He} = 80\%$. It is seen that $T$ as well as $P$ for $^3$He vary significantly across the assumed wavelength band. In contrast, based on the transmission data shown in Fig. 3 and assuming that tWAPAs perform similarly as polarizing V- or Z-cavities [26,28] we expect achieving easily a rather $\lambda$-independent polarization and transmission for tWAPAs well above 90% and 30%, respectively. For completeness we note that bending of the Si substrates may lead to a decrease of the transmission due to Laue-extinction. However, as shown by Stunault et al. [29], Laue-extinction seems to be small.

We abstain from a more detailed discussion about the performance of $^3$He-cells and tWAPAs, because of the very wide range of applications of wide-angle spin analysis. $^3$He-cells have the advantage that they can be placed very close to the sample thus yielding spin analysis over a very large solid angle, while WAPAs restrict the vertical divergence to $5^0 - 10^0$. For example, for POLANO at MLF, the vertical divergence is $8^0$ [20]. Note that in many experiments, cryomagnets are used, which restrict the vertical divergence too.

**Table 1**
Comparison of the polarization $P$ and transmission $T$ of a tWAPA with a $^3$He spin filter cell. Its parameters are $l = 3$ cm, $p = 2.5$ bar, and $p_{He} = 80\%$ (see Eq. (11)). $P^2T$ designates the quality factor. In our notation it can attain a maximum value of 0.5 because we consider the transmission of unpolarized neutrons through the polarizer.

| Device | $\lambda$ (Å) | $P$ | $T$ | $P^2T$ |
|---|---|---|---|---|
| $^3$He | 2 | 0.71 | 0.47 | 0.23 |
| $^3$He | 5 | 0.98 | 0.29 | 0.28 |
| $^3$He | 10 | 1.00 | 0.17 | 0.167 |
| $^3$He | 14.8 | 1.00 | 0.10 | 0.098 |
| tWAPA | 2–14.8 | >0.9 | >0.3 | >0.24 |

## 4. Conclusions

We have described the design of a wide-angle polarization analyzer (WAPA) that uses the polarizing mirrors in transmission geometry (tWAPA), i.e. the spin-down neutrons pass the supermirror coating while the spin-up neutrons are reflected out and absorbed. Therefore, in contrast to the majority of reflection WAPAs presently used [8,16,20], the phase space of the transmitted neutrons is not affected by the polarizing mirrors. Moreover, warping of the polarizing substrates has no strong impact on the performance of the WAPA, i.e. the associated increased waviness reduces only the bandwidth of the analyzer.

In contrast to WAPAs operated in reflection, where typically 20%–40% of the polarized neutrons are absorbed by the absorbing substrates, the transmission of the tWAPA suffers only from the absorption of the neutrons by the Si substrates and the polarizing coatings. Therefore, the transmission of the spin-down neutrons will be comparable to polarizing cavities. In addition, we have shown that the bandwidth $Q_P$ is enlarged when compared with conventional designs [23] using flat mirrors, i.e. for small samples and perfect geometry, $Q_P$ can be quantified by the ratio $Q_P = m_{max}/m_{min} = \lambda_{min}/\lambda_{max}$. For supermirror with $m = 5$ one obtains for an ideal geometry and small samples $Q_P = 7.4$. With the availability of polarizing mirrors with $m = 7$, $Q_P$ can be increased to approximately 10.

Finally, let us summarize some additional advantages offered by the transmission geometry: The tWAPA can be designed simply by using analytical calculations that can be extended to respect a finite sample size in a straightforward way. The polarization of the transmitted neutrons can be improved by doubling or even tripling the number of polarizing blades reducing the transmission of the tWAPA only slightly [28]. The separation of the collimating from the polarizing section allows adjusting the momentum resolution of the tWAPA by inserting different radial collimators. The concept of the tWAPA may also be used for polarizing strongly converging neutron beams for example before the sample position.

### Declaration of competing interest

The authors declare that they have no known competing financial interests or personal relationships that could have appeared to influence the work reported in this paper.

### CRediT authorship contribution statement

**Peter Böni:** Writing - original draft. **Christian Schanzer:** review & editing. **Michael Schneider:** review & editing.

### Appendix A. tWAPA Using Z-cavities

Fig. A.7 shows the basic design of the tWAPA using Z-cavities. The neutrons are scattered from a cylindrical sample that has a diameter $d$ (typically 10 mm). The neutrons with spin down are transmitted through the polarizing blades, which are shown as green lines. To absorb the spin-up neutrons and to avoid cross talk between the channels, a radial collimator is placed outside the area of the polarizing blades,

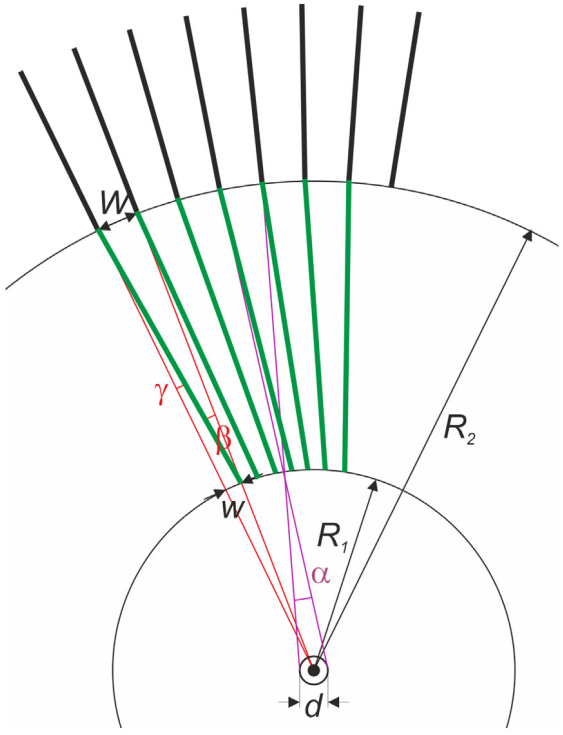


**Fig. A.7.** Design of the tWAPA using flat substrates. The width of the channels at the entrance and exit of the polarizing section are $w$ and $W$, respectively. The entrance and exit are located on a circle with radius $R_1$ and $R_2$. The diameter of the cylindrical sample is $d$.

i.e. in the area $R > R_2$. The blades are made so long that no wrongly polarized neutrons can reach the detector.

The widths $w$ and $W$ are related to each other by

$$\frac{W}{w} = \frac{R_2}{R_1}. \tag{A.1}$$

According to Fig. A.7, the divergence of the beam is given by

$$\alpha = \frac{d + W}{R_2} \tag{A.2}$$

if the collimating blades have the same angular separation as the polarizing blades. Of course, the angular resolution can be improved by reducing the angular separation of the collimating blades.

The maximum angle of reflection is determined by a contribution from the width of the channel at the exit, $W$, and the diameter of the sample, $d$

$$\beta_{max} = \beta + \frac{d/2}{R_1} = \frac{W}{R_2 - R_1} + \frac{d}{2R_1}. \tag{A.3}$$

Similarly, the minimum angle of reflection is given by

$$\gamma_{min} = \gamma - \frac{d/2}{R_1} = \frac{w}{R_2 - R_1} - \frac{d}{2R_1}. \tag{A.4}$$

Neutrons with spin up are reflected from the polarizing mirrors for angles of reflection $\theta_c^{dn} \leq \psi \leq \theta_c^{up}$, where $\theta_c^{dn} = cm_{min}\lambda$ and $\theta_c^{up} = cm_{max}\lambda$. The supermirror parameters $m_{min}$ and $m_{max}$ are determined by the properties of the supermirror, i.e. according to the example shown in Fig. 3, $m_{min} = 0.68$ and $m_{max} = 5.0$. Therefore, one obtains for the lower critical wavelength

$$\lambda_{min} \geq \frac{\beta_{max}}{cm_{max}} \tag{A.5}$$

and for the upper critical wavelength

$$\lambda_{max} \geq \frac{\gamma_{min}}{cm_{min}}. \tag{A.6}$$

For an efficient use of the TOF technique, a wide range of wavelengths for which the tWAPA polarizes the neutrons is important, i.e. a large ratio $\lambda_{max}/\lambda_{min}$ is of advantage. According to Eqs. (A.5) and (A.6) one obtains

$$Q_P = \frac{\gamma_{min} m_{max}}{\beta_{max} m_{min}}. \tag{A.7}$$

For a vanishing sample size ($d = 0$), Eq. (A.7) yields together with Eqs. (A.3), (A.4), and Eq. (A.2)

$$Q_P(d=0) = \frac{w m_{max}}{W m_{min}} = \frac{R_1 m_{max}}{R_2 m_{min}}. \tag{A.8}$$

For a typical design of a WAPA with $R_1 = 1000$ mm, $R_2 = 1500$ mm, $m_{min} = 0.68$, and $m_{max} = 5.0$ one obtains

$$Q_P^{ex} = 4.9. \tag{A.9}$$

## References


[1] R.M. Moon, T. Riste, W.C. Koehler, Polarization analysis of thermal-neutron scattering, Phys. Rev. 181 (1969) 920–931, http://dx.doi.org/10.1103/PhysRev.181.920, https://link.aps.org/doi/10.1103/PhysRev.181.920.

[2] G. Shirane, R. Cowley, C. Majkrzak, J.B. Sokoloff, B. Pagonis, C.H. Perry, Y. Ishikawa, Spiral magnetic correlation in cubic MnSi, Phys. Rev. B 28 (1983) 6251–6255, http://dx.doi.org/10.1103/PhysRevB.28.6251, https://link.aps.org/doi/10.1103/PhysRevB.28.6251.

[3] K.R.A. Ziebeck, P.J. Brown, Measurement of the paramagnetic response function in the weak itinerant magnetic compound MnSi using polarised neutron scattering, J. Phys. F: Metal Phys. 10 (9) (1980) 2015–2024, http://dx.doi.org/10.1088/0305-4608/10/9/017.

[4] O. Schaerpf, Properties of beam bender type neutron polarizers using supermirrors, Physica B 156–157 (1989) 639–646, http://dx.doi.org/10.1016/0921-4526(89)90751-5, http://www.sciencedirect.com/science/article/pii/0921452689907515.

[5] F. Mezei, Novel polarized neutron devices: supermirror and spin component amplifier, Commun. Phys. 1 (1976) 81–85.

[6] F. Mezei, P.A. Dagliesh, Corrigendum and first experimental evidence on neutron supermirrors, Commun. Phys. 2 (1977) 41–43.

[7] P. Böni, Supermirror-based beam devices, in: Proceedings of the First European Conference on Neutron Scattering, Physica B 234–236 (1997) 1038–1043, http://dx.doi.org/10.1016/S0921-4526(96)01255-0, http://www.sciencedirect.com/science/article/pii/S0921452696012550.

[8] O. Schärpf, Polarization analysis techniques for quasielastic neutron scattering, Physica B 182 (4) (1992) 376–388, Quasielastic Neutron Scattering. http://dx.doi.org/10.1016/0921-4526(92)90041-P. http://www.sciencedirect.com/science/article/pii/092145269290041P.

[9] W. Schweika, P. Böni, The instrument DNS: polarization analysis for diffuse neutron scattering, in: Proceeding of the Third International Workshop on Polarised Neutrons, Physica B 297 (1) (2001) 155–159, http://dx.doi.org/10.1016/S0921-4526(00)00858-9, http://www.sciencedirect.com/science/article/pii/S0921452600008589.

[10] SNS, SNS Website, 2019, URL http://neutrons.ornl.gov/facilities/SNS/.

[11] ISIS, ISIS Website, 2019, URL http://www.isis.stfc.ac.uk.

[12] JPARC, JPARC Website, 2019, URL http://www.j-parc.jp/index-e.html.

[13] ESS, ESS Website, 2019, URL http://www.europeanspallationsource.se.

[14] T.R. Gentile, P.J. Nacher, B. Saam, T.G. Walker, Optically polarized $^3$He, Rev. Modern Phys. 89 (2017) 045004, http://dx.doi.org/10.1103/RevModPhys.89.045004, https://link.aps.org/doi/10.1103/RevModPhys.89.045004.

[15] Barry Winn, Uwe Filges, V. Ovidiu Garlea, Melissa Graves-Brook, Mark Hagen, Chenyang Jiang, Michel Kenzelmann, Larry Passell, Stephen M. Shapiro, Xin Tong, Igor Zaliznyak, Recent progress on HYSPEC, and its polarization analysis capabilities, EPJ Web Conf. 83 (2015) 03017, http://dx.doi.org/10.1051/epjconf/20158303017, https://doi.org/10.1051/epjconf/20158303017.

[16] I.A Zaliznyak, A.T. Savici, V. Ovidiu Garlea, B. Winn, U. Filges, J. Schneeloch, J.M. Tranquada, G. Gu, A. Wang, C. Petrovic, Polarized neutron scattering on HYSPEC: the HYbrid SPECtrometer at SNS, 2016, ArXiv e-prints, arXiv:1610.06018.

[17] T. Yokoo, K. Ohoyama, S. Itoh, J. Suzuki, M. Nanbu, N. Kaneko, K. Iwasa, T.J. Sato, H. Kimura, M. Ohkawara, Construction of polarized inelastic neutron spectrometer in J-PARC, J. Phys. Conf. Ser. 502 (1) (2014) 012046, http://stacks.iop.org/1742-6596/502/i=1/a=012046.

[18] K. Ohoyama, T. Yokoo, S. Itoh, T. Ino, M. Ohkawara, T. Oku, S. Tasaki, K. Iwasa, T.J. Sato, S. Ishimoto, K. Taketani, H. Kira, Y. Sakaguch, M. Nanbu, H. Hiraka, H.M. Shimizu, M. Takeda, M. Hino, K. Hayashi, U. Filges, P. Hautle, Concepts of neutron polarisation analysis devices for a new neutron chopper spectrometer, POLANO, in J-PARC, J. Phys. Conf. Ser. 502 (1) (2014) 012051, http://stacks.iop.org/1742-6596/502/i=1/a=012051.

[19] K. Ohoyama, T. Yokoo, S. Itoh, M. Nanbu, Kazuaki Iwasa, M. Ohkawara, N. Kaneko, T. Ino, H. Hayashida, Tsuneyuki Oku, H. Kira, S. Tasaki, M. Takeda, H. Kimura, Taku Sato, Polarisation analysis neutron spectrometer, POLANO, at J-PARC - Concept and magnetic field optimisation, J. Phys. Conf. Ser. 711 (2016) 012010.

[20] M. Schneider, C. Schanzer, P. Böni, In review at NIMA, 2020.

[21] C. Pappas, G. Kali, T. Krist, P. Böni, F. Mezei, Wide angle NSE: the multidetector spectrometer SPAN at BENSC, Physica B 283 (4) (2000) 365–371, http://dx.doi.org/10.1016/S0921-4526(00)00341-0, http://www.sciencedirect.com/science/article/pii/S0921452600003410.

[22] Peter Fouquet, Georg Ehlers, Bela Farago, Catherine Pappas, Ferenc Mezei, The wide-angle neutron spin echo spectrometer project WASP, J. Neutron Res. 15 (1) (2007) 39–47, http://dx.doi.org/10.1080/10238160601048791, http://www.tandfonline.com/doi/abs/10.1080/10238160601048791, arXiv:http://www.tandfonline.com/doi/pdf/10.1080/10238160601048791.

[23] T. Krist, F. Mezei, Neutron optical developments at HMI berlin, Proc. ICANS-XVIII (2007) 149–155, ; 18th Meeting of the International Collaboration on Advanced Neutron Sources, April 25-29, Dongguan, Guangdong, P. R. China.

[24] SwissNeutronics, Swissneutronics website, 2019, URL https://www.swissneutronics.ch/products/neutron-supermirrors.

[25] Jochen Stahn, Artur Glavic, Efficient polarization analysis for focusing neutron instruments, J. Phys. Conf. Ser. 862 (2017) 012007, http://dx.doi.org/10.1088/1742-6596/862/1/012007.

[26] C. Schanzer, M. Schneider, P. Böni, Neutron optics: Towards applications for hot neutrons, J. Phys. Conf. Ser. 746 (1) (2016) 012024, URL http://stacks.iop.org/1742-6596/746/i=1/a=012024.

[27] W. Heil, K.H. Andersen, R. Cywinski, H. Humblot, C. Ritter, T.W. Roberts, J.R. Stewart, Large solid-angle polarisation analysis at thermal neutron wavelengths using a 3he spin filter, Nucl. Instrum. Methods Phys. Res. A 485 (3) (2002) 551–570, http://dx.doi.org/10.1016/S0168-9002(01)00926-3, http://www.sciencedirect.com/science/article/pii/S0168900201009263.

[28] P. Böni, W. Münzer, A. Ostermann, Instrumentation with polarized neutrons, Physica B 404 (17) (2009) 2620–2623, http://dx.doi.org/10.1016/j.physb.2009.06.031, http://www.sciencedirect.com/science/article/pii/S0921452609003895.

[29] A. Stunault, K.H. Andersen, S. Roux, T. Bigault, K. Ben-Saidane, H.M. Rønnow, New solid state polarizing bender for cold neutrons, Physica B 385–386 (2006) 1152–1154, http://dx.doi.org/10.1016/j.physb.2006.05.396, http://www.sciencedirect.com/science/article/pii/S0921452606012877.